Carbohydrate Polymers 110 (2014) 163–172

Contents lists available at ScienceDirect

Carbohydrate Polymers

journal homepage: www.elsevier.com/locate/carbpol

Modification of nanofibrillated cellulose using amphiphilic block-structured galactoglucomannans

Alina Lozhechnikova[a,1], Daniel Dax[b,*,1], Jari Vartiainen[c], Stefan Willför[b], Chunlin Xu[b,d], Monika Österberg[a,**]

[a] Department of Forest Products Technology, School of Chemical Technology, Aalto University, P.O. Box 16300, FI-0076 Aalto, Finland
[b] Process Chemistry Centre, c/o Laboratory of Wood and Paper Chemistry, Åbo Akademi University, Porthansgatan 3, FI-20500 Åbo/Turku, Finland
[c] VTT Technical Research Centre of Finland, Biologinkuja 7, P.O. Box 1000, FI-02044 Espoo, Finland
[d] Wallenberg Wood Science Center, KTH, The Royal Institute of Technology, SE-10044 Stockholm, Sweden

ARTICLE INFO

Article history:
Received 21 February 2014
Received in revised form 25 March 2014
Accepted 26 March 2014
Available online 4 April 2014

Keywords:
NFC
CNF
O-Acetyl galactoglucomannan
Fatty acid
Amphiphilic
QCM-D

ABSTRACT

Nanofibrillated cellulose (NFC) and hemicelluloses have shown to be highly promising renewable components both as barrier materials and in novel biocomposites. However, the hydrophilic nature of these materials restricts their use in some applications. In this work, the usability of modified *O*-acetyl galactoglucomannan (GGM) for modification of NFC surface properties was studied. Four GGM-block-structured, amphiphilic derivatives were synthesized using either fatty acids or polydimethylsiloxane as hydrophobic tails. The adsorption of these GGM derivatives was consecutively examined in aqueous solution using a quartz crystal microbalance with dissipation monitoring (QCM-D). It was found that the hydrophobic tails did not hinder adsorption of the GGM derivatives to cellulose, which was concluded to be due to the presence of the native GGM-block with high affinity to cellulose. The layer properties of the adsorbed block-co-polymers were discussed and evaluated. Self-standing NFC films were further prepared and coated with the GGM derivatives and the effect of the surface modification on wetting properties and oxygen permeability (OP) of the modified films was assessed.

1. Introduction

In the last decades huge efforts have been made to develop new materials applying biorenewable resources in order to replace widely used oil-based products. The depletability of oil-based starting materials, as well as big cost fluctuations and uneven regional occurrence of crude oil leads to a rising industrial interest to find alternatives. Together with the progresses in processing plant materials such as starch, lignin, cellulose, and hemicelluloses these let forecast that more and more everyday products will be partially or completely composed of biodegradable or biorenewable materials. From the abovementioned plant materials especially cellulose and hemicelluloses have promising properties such as their high abundance, as well as the already existing refining factories such as pulp mills. Furthermore, the use of cellulose and hemicelluloses do not rise ethical issues because they cannot be used as food, which makes them favorable compared to starch. One promising water-soluble hemicellulose is *O*-acetyl galactoglucomannan (GGM), which can be extracted from wood by pressurized hot-water extraction (PHWE) (Al Manasrah, Kallioinen, Ilvesniemi, & Manttari, 2012) or recovered from the wastewaters of the thermomechanical pulping process by ultrafiltration (Lundqvist, Jacobs, Palm, Zacchi, Dahlman, & Stålbrand, 2003; Willför, Sjöholm, Laine, Roslund, Hemming, & Holmbom, 2003). GGM consists of a linear backbone of randomly distributed (1 → 4)-linked β-D-mannopyranosyl (Man*p*) and (1 → 4)-linked β-D-glucopyranosyl (Glc*p*) units, with α-D-galactopyranosyl (Gal*p*) units as single side units (Hannuksela & Hervé du Penhoat, 2004). GGM is partially acetylated and the *O*-acetyl groups are located randomly at C2 and C3 position of the mannose units in the main chain (Willför, Sjöholm, Laine, Roslund, Hemming, & Holmbom, 2003). Native GGM has been modified in several ways, e.g. by substitution of the hydroxyl groups (Albertsson, Voepel, Edlund, Dahlman, & Söderqvist-Lindblad, 2010; Kisonen et al., 2012; Voepel, Edlund, Albertsson, & Percec, 2011) of the polysaccharide chain or recently also by reductive amination of the reducing end of GGM (Dax, Eklund, et al., 2013; Dax, Xu, et al., 2013).

* Corresponding author. Tel.: +358 22154886
** Corresponding author. Tel.: +358 505497218.
E-mail addresses: ddax@abo.fi (D. Dax), monika.osterberg@aalto.fi (M. Österberg).
[1] These authors contributed equally to this work.

http://dx.doi.org/10.1016/j.carbpol.2014.03.087
0144-8617/

Nanofibrillated cellulose (NFC) or cellulose nanofibrils (CNF), is a relatively new cellulose form in which the cellulose fibers have a width in nanoscale. It can be produced by bacteria (Yamanaka, Watanabe, & Kitamura, 1989) and is then called bacterial cellulose, or from plant sources by disintegration of the cellulose fibers (NFC). Recent developments allow the production of NFC from wood fibers at relatively low energy consumption and the obtained NFC features a combination of high aspect ratio, high specific surface area as well as a high strength and flexibility (Pääkkö et al., 2007). Furthermore NFC shows non-toxicity, biodegradability, and biocompatibility, which makes various areas of application possible (Klemm, Heublein, Fink, & Bohn, 2005). The hydrophilicity of NFC is a challenge for some applications, for example the implementation of NFC in composites (Svagan, Azizi Samir, & Berglund, 2007), and thus modifications of NFC are often necessary (Hubbe, Rojas, Lucia, & Sain, 2008). This can be achieved by targeting the hydroxyl groups at the NFC surface in chemical reactions such as silylation for hydrophobization of the NFC (Andresen & Stenius, 2007), esterification to introduce groups with antimicrobial properties (Andresen et al., 2007), or initiator groups for controlled radical polymerizations (Lacerda, Barros-Timmons, Freire, Silvestre, & Neto, 2013). These mentioned grafting reactions lead to new NFC derivatives with interesting properties, but they all require solvent exchange from water to a suitable organic solvent, which is not only time and solvent consuming but may lead to aggregation of the NFC (Johansson, Tammelin, Campbell, Setälä, & Österberg, 2011). As a consequence, intensive efforts are made to modify the NFC surface using water as a solvent. For example a cerium (IV) induced polymerization was performed introducing polymer chains with an undefined chain length to the NFC surface (Littunen et al., 2011; Stenstad, Andresen, Tanem, & Stenius, 2008).

Instead of direct chemical modification of the cellulose backbone, adsorption of polymers or surfactants have been applied to overcome the problem of solvent exchange (Moon, Martini, Nairn, Simonsen, & Youngblood, 2011). This approach is in general easier to apply since the polymer or surfactant can be synthesized prior to use without any solvent restrictions and then be added to the NFC in aqueous media. Cationic polymers have been used especially to modify the surface of highly anionic NFC (Taipale, Österberg, Nykänen, Ruokolainen, & Laine, 2010; Wågberg et al., 2008; Wang et al., 2011), whereas for the modification of unmodified low-charged NFC, hemicelluloses and cellulose derivatives have been used due to their natural affinity toward NFC. Different approaches using carboxymethyl cellulose for the modification of the NFC surface have been reported (Filpponen et al., 2012; Olszewska et al., 2013), but the negative charge of carboxymethyl cellulose was found to be obstructive for a high adsorption on NFC. By contrast it has been reported that e.g. unmodified hemicelluloses like xyloglucans, arabinoxylans, and GGM can adsorb in considerable amounts to NFC (Eronen, Österberg, Heikkinen, Tenkanen, & Laine, 2011) and hence are promising starting materials for its modification. Compared to the unmodified GGM, GGM bearing carboxyl groups in the main chain showed a diminished adsorption to NFC (Parikka et al., 2012). This leads to the assumption that with increasing modification of the main chain of GGM its sorption capacities decrease. In order to use GGM as a carrier of functional groups for the modification of NFC, the main chain of GGM should preserve its native structure. Different ways for the synthesis of block-structured and amphiphilic polysaccharides derivatives based on dextran, chitosan or xyloglucan are described in literature (Schatz & Lecommandoux, 2010). The synthesis of block-structured GGMs has been recently reported, applying coupling reactions (Dax, Eklund, et al., 2013; Dax, Xu, et al., 2013) or controlled radical polymerization (Dax, Eklund, et al., 2013; Dax, Xu, et al., 2013). These GGM derivatives are of high interest because the GGM chain preserves its native structure in respect to molar mass, composition and degree of acetylation, and hence the block-structured GGMs are likely to reveal high affinity to celluloses.

During the past years Quartz Crystal Microbalance with Dissipation monitoring (QCM-D) has been intensively used to study adsorption of various biomaterials to cellulose and recently also NFC has been intensively studied as a substrate (Wågberg, Enarsson, & Österberg, 2010). It is not only possible to follow adsorption in real time using this method, but also to determine the amount of substance adsorbed and to follow the changes in viscoelasticity of the formed film.

In this paper we describe the synthesis of block-structured GGM derivatives in which the GGM main chain preserved its native structure and only the reducing end was modified. Native GGM and its derivatives were analyzed by proton and carbon NMR techniques, as well as by FTIR. The possibility to use synthesized amphiphilic derivatives for NFC modification was investigated, and their adsorption on ultrathin NFC films was extensively studied using QCM-D. Furthermore, self-standing NFC films were coated with GGM and the amphiphilic GGM derivatives and the effect of this modification on wetting and oxygen permeability was explored.

2. Experimental

2.1. Chemicals

Di-*tert*-butyl-dicarbonate (Aldrich), ethylenediamine (EDA) ≥99.5% (Aldrich), sodium cyanoborohydride 95% (Aldrich), 1,1′-carbonyldiimidazole (CDI) 97% (Aldrich), trifluoroacetic acid (TFA) 99% (Aldrich), pelargonic acid ≥97% (Fluka), myristic acid 99.5% (Fulka), stearic acid 99% (Merck), bis(3-aminopropyl) terminated poly(dimethlsiloxane) (NH_2-PDMS-NH_2) (ABCR), dimethyl sulfoxide (DMSO) (Merck), ethanol ≥99.5 vol.% (Altia Oyj), acetone (J.T. Baker), tetrahydrofuran (THF) (J.T. Baker), 1,4-dioxane (VWR) are available commercially and were reagent grade or better and used without further purification. Hot-water extracted *O*-acetyl galactoglucomannan (GGM) from Norway spruce (*Picea abies*) was provided by The Finnish Forest Research Institute – Metla. GGM was obtained as a solution with concentration of 30 wt.%. The extract was further purified in order to remove impurities and to narrow down the molar mass distribution (low polydispersity (PDI)). Therefore, the concentrated GGM solution (330 ml) was diluted with water (670 ml) and then precipitated in 9 l of ethanol at room temperature. The colorless precipitate was filtrated off and consecutively washed with ethanol, acetone, and methyl *tert*-butyl ether and finally the solid GGM was freeze-dried. The purified GGM had a weight average molar mass (M_w) of 7.1×10^3 g/mol and a number average molar mass (M_n) of 4.7×10^3 g/mol (polydispersity ~ 1.5), as determined by High Pressure Size Exclusion Chromatography (HPSEC). The sugar ratio of GGM was determined by acid methanolysis and was around 5–4:1:0.5–1.1 (Man:Glc:Gal) and the degree of acetylation (DS_{Ac}) ~ 0.20.

2.2. Nanofibrillated cellulose films

The cellulose nanofibrils were prepared from never-dried industrial pulp in the Finnish Centre for Nanocellulosic Technologies. Bleached hardwood kraft pulp was washed into sodium form (Swerin, Ödberg, & Lindström, 1990) in order to control both the counterion type and ionic strength. A high-pressure fluidizer (Microfluidics, M-110Y, Microfluidics Int. Co., Newton, MA) was used to disintegrate the washed pulp. NFC used for self-standing films and for QCM measurements was disintegrated in the fluidizer for 6 and 20 passes, respectively. No chemical or enzymatic pretreatment was applied prior to disintegration.

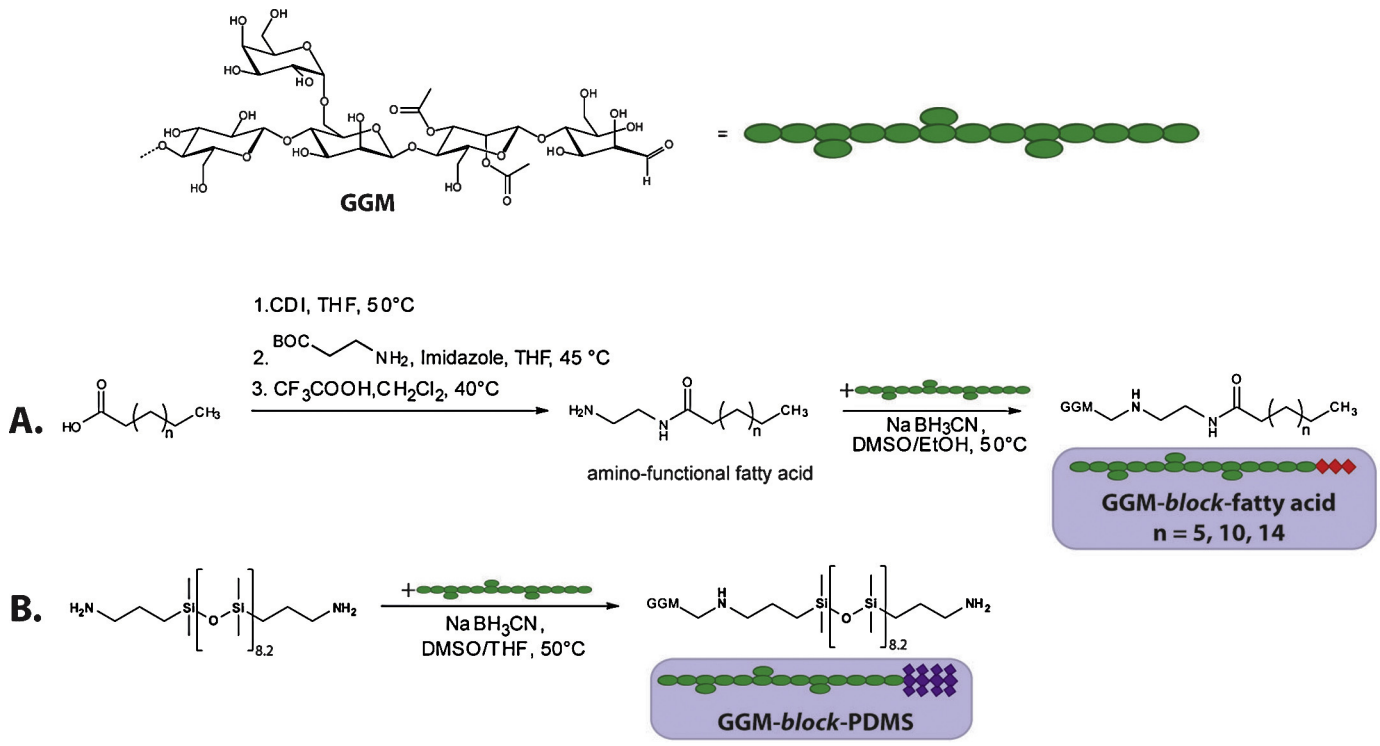

Scheme 1. Reaction conditions for the synthesis of GGM-*block*-fatty acid (A) (Dax, Eklund, et al., 2013; Dax, Xu, et al., 2013) and the synthesis of GGM-*block*-PDMS derivatives (B). Schematic illustrations of the respective products are also shown.

Self-standing NFC films were prepared by pressurized filtration. To produce one film, 110 ml of 0.84% NFC suspension was used. After filtration, films were wet-pressed in a Carver Laboratory press (Fred S. Carver Inc.) at 100 °C and 1800 Pa for 2 h. Films were stored at 23 °C and 50% relative humidity for at least 48 h prior to modification or further measurements. The thickness of the films was measured using a Lorenz Wetter paper thickness meter. Thickness of each sample was measured at least three times. More detailed information about NFC and production of NFC films can be found elsewhere (Österberg et al., 2013).

For oxygen permeability and contact angle measurements, the NFC films (d = 12 cm) were cut to 3 cm × 3 cm size, spin-coated (1 min, 4000 rpm) with 7 g/l GGM or GGM derivatives solution, and dried in hot press for 30 min (80 °C, 5 kg/cm^2).

In order to prepare ultrathin films from NFC, a previously developed (Ahola, Salmi, Johansson, Laine, & Österberg, 2008) and optimized procedure (Eronen et al., 2011) was adopted. 1.3% NFC gel was diluted to 1.67 g/l concentration with extra purified deionized Milli-Q water (Millipore synergy UV, Millipore, S.A.S., Molsheim, France). To remove fibril aggregates, the suspension was ultrasonicated using a micro tip (Branson Digital Sonfire s-4500, Branson Corp., Danburg, CT) for 10 min at 25% amplitude, and centrifuged (Optima L-90K ultracentrifuge, Beckman Coulter, USA) at 10400 rpm for 45 min. Clear upper supernatant phase (~1.2 g/l) was collected in order to use the nanosized fraction only. Silica covered QCM-D crystals (Q-Sense AB, Gothenburg, Sweden) with an anchoring layer of polyethylene imine (PEI) were used as substrates for spin-coating of NFC (1 min, 3000 rpm).

2.3. Synthesis of GGM-block-copolymers

Two different types of GGM-block-structured derivatives were synthesized in order to generate biobased amphiphilic products. The hydrophobic block was either fatty acid or polydimethylsiloxane (PDMS).

2.3.1. Synthesis of GGM-block-fatty acid

In this approach three different fatty acids were converted into amino functional fatty acids and consecutively reacted with GGM in a reductive amination resulting in block structured GGM derivatives (Scheme 1). The reaction parameters have been described earlier (Dax, Eklund, et al., 2013; Dax, Xu, et al., 2013) and are summarized in the supporting information.

2.3.2. Synthesis of GGM-block-PDMS

For the reductive amination of GGM with NH_2-PDMS-NH_2, a 20-fold excess of the NH_2-PDMS-NH_2 was used to assure the formation of AB-block structured derivatives and avoid the formation of ABA block structured derivatives. GGM (5 g, 1.05 mmol, 1 equiv.) was dissolved in 125 ml of DMSO and the temperature was adjusted to 50 °C. A solution of NH_2-PDMS-NH_2 (18.95 g, 21.05 mmol, 20 equiv.) in 50 ml of THF was prepared and the amine groups were protonated using aqueous H_2SO_4. Consecutively, the NH_2-PDMS-NH_2 solution was quickly added to the GGM and the pH was verified to be around 4. After stirring for 1 h at 50 °C, $NaBH_3CN$ (3.31 g, 52.7 mmol, 50 equiv.) was introduced to the homogenous reaction mixture and the stirring was continued at a high speed for 24 h. Then a second addition of $NaBH_3CN$ (3.31 g, 52.7 mmol, 50 equiv.) was performed in order to ensure complete conversion of all the GGM reducing ends. After 24 h additional stirring at 50 °C the reaction mixture was precipitated in 700 ml of ethanol. The product was filtered off and redissolved in distilled water and precipitated a second time in EtOH in order to remove unreacted residues of NH_2-PDMS-NH_2. Consecutively, the product was dissolved in a small amount of distilled water and dialyzed (cut-off 2 kDa) against distilled water for 48 h while the water was renewed every 12 h. Finally, the solution was freeze-dried to result in a white solid (3.17 g, 0.55 mmol, 56% yield). ^{1}H NMR (D_2O, 25 °C, ppm): δ-0.18–0.23 (56H, m, Si—CH_3), 0.55 (2H, t, Si—CH_2—$(CH_2)_2$—NH_2), 0.56 (2H, t, and Si—CH_2—$(CH_2)_2$—NH—), 1.71 (2H, m, Si—CH_2—CH_2—CH_2—NH_2),

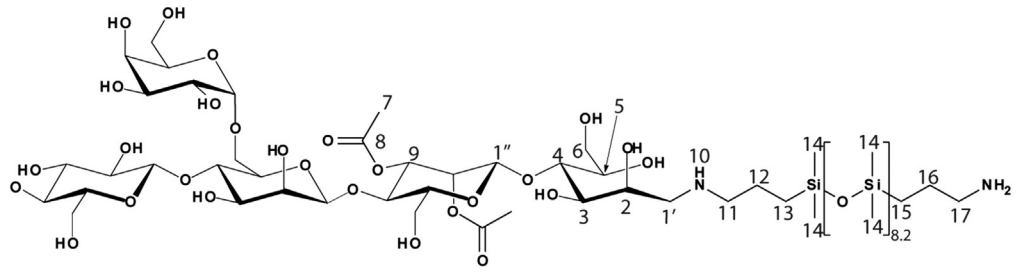

GGM-*block*-PDMS

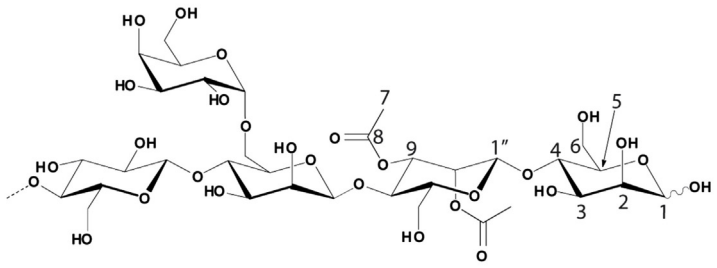

native GGM

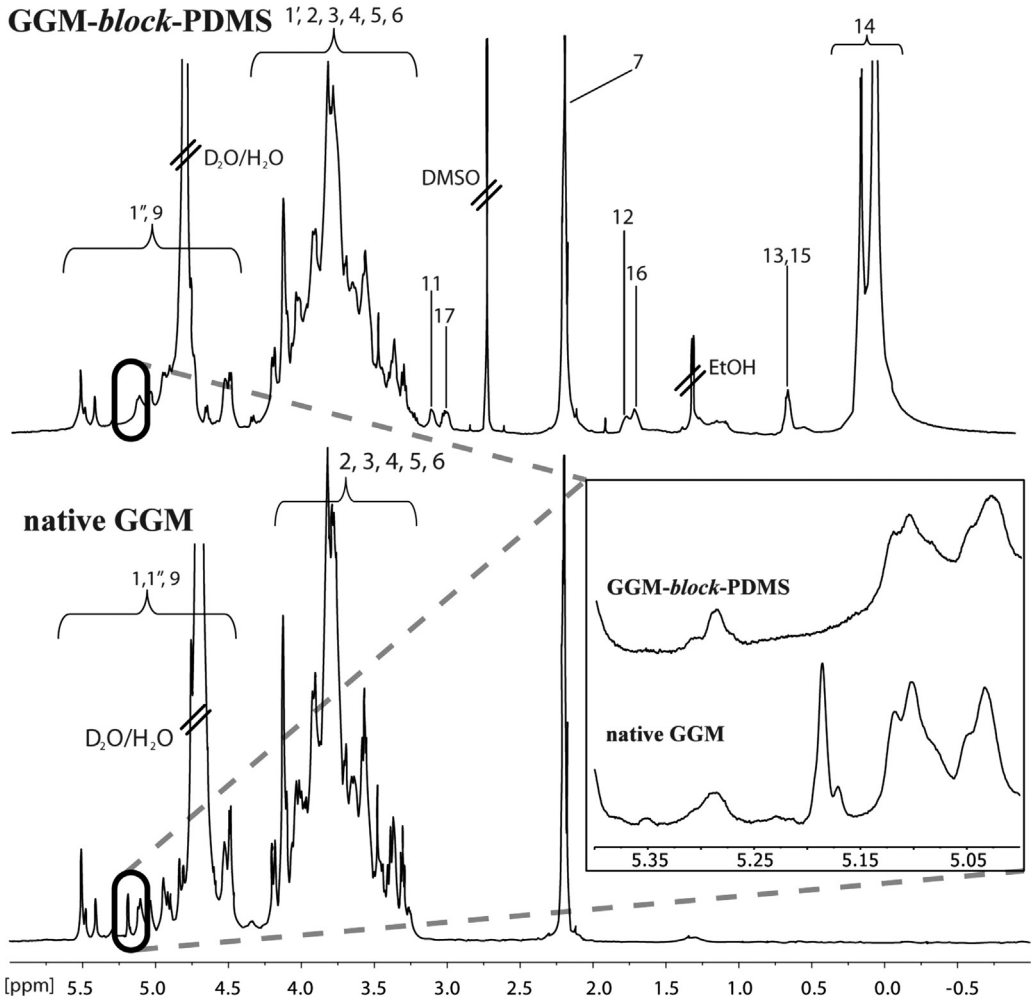

Fig. 1. ^{1}H NMR spectra of native GGM and its block-structured derivative. In the inset the reducing end peak region of GGM is highlighted and the complete disappearance of the reducing end peak can be observed for the GGM-*block*-PDMS.

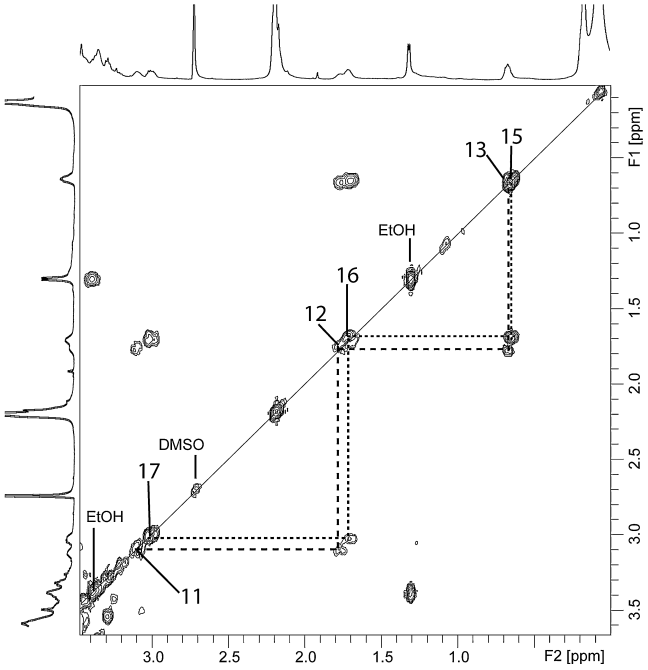

Fig. 2. COSY spectrum of the GGM-*block*-PDMS derivative.

1.77 (2H, m, Si—CH_2—CH_2—CH_2—NH—), 3.01 (2H, m, Si—$(CH_2)_2$—CH_2—NH_2), 3.12 (2H, m, Si—$(CH_2)_2$—CH_2—NH—). The complete peak assignment can also be found in Fig. 1 (^{1}H spectra). Because the different signals of the PDMS derivative could not be separately assigned only using ^{1}H NMR, a 2D spectrum (COSY) of the product was recorded and evaluated (Fig. 2).

2.4. Nuclear magnetic resonance spectroscopy (NMR)

The native GGM and the GGM derivatives were analyzed by ^{1}H and ^{13}C NMR measurements using a Bruker Avance spectrometer (operation frequency: ^{1}H: 600.13 MHz; ^{13}C: 150.92 MHz). All the samples were soluble in water and D_2O was used as a solvent.

2.5. Fourier transformed infrared spectroscopy (FTIR)

The infrared spectroscopy measurements were performed with a Bruker ALPHA series using the ALPHA platinum ATR single reflection diamond ATR module. The samples were directly placed on the ATR plate for measurement. The results were evaluated using the software OPUS from Bruker.

2.6. Determination of the surface tension in water

The surface tension of the solutions of the amphiphilic GGM derivatives was measured by the Du Noüy ring method using a KSV Sigma 70 Tensiometer. The used Pt-Ir ring was rinsed with ethanol with consecutive drying after each measurement to ensure zero contact angle. The real tension values were immediately determined for different concentrations of the surfactants at 25 °C. The equilibrium time for all the samples was set to 5 min. The surface tensions were plotted versus the logarithm of the surfactant concentration (mg/ml) and the respective critical micelle concentrations (CMC) were determined graphically from the drastic change of the slope.

2.7. Quartz crystal microbalance with dissipation monitoring

The in situ adsorption of GGM and its derivatives on ultrathin NFC films was monitored using a QCM-D instrument (E4, Q-Sense AB, Västra Frölunda, Sweden). The technique is based on the changes in oscillation of a quartz crystal caused by changes in mass. With E4 instrument, changes in frequency and dissipation energy (frictional losses due to viscoelastic properties of the adsorbed layer, ΔD) can be monitored simultaneously. During adsorption the oscillation frequency of the crystal increases and deviation from the fundamental frequency (5 MHz) and its overtones (15, 25, 35, 55, and 75 MHz) is detected. According to the Sauerbrey equation (1) (Sauerbrey, 1959), the change in frequency (Δf) is proportional to the mass adsorbed per unit surface (Δm),

$$\Delta m = \frac{-c\Delta f}{n} \quad (1)$$

where C is the sensitivity constant (here $C = 0.177\ \mathrm{mg/m^2}$) and n is the overtone number (here $n = 3$). Eq. (1) is valid for thin, rigid, and uniform films, but it underestimates mass for viscoelastic films, when $\Delta D > 1$ (Höök, Kasemo, Nylander, Fant, Sott, & Elwing, 2001). Therefore the calculated mass values presented here are estimations and should not be used as absolute values. GGM and derivatives were dissolved in pure water to 0.5 g/l concentration. The flow rate through the QCM-D chambers was set to 0.1 ml/min and kept constant during measurements.

2.8. Oxygen transmission rate (OTR)

The measurements were performed with Oxygen Permation Analyser Models 8001 and 8011 (Systech Instruments Ltd., UK) with two replicates. The tests were carried out at 23 °C temperature and 0% and 80% relative humidity using metal masks with a test area of 5 cm^2. The coated side of the samples faced the test gas (100% oxygen). OP was calculated by multiplying OTR value by the thickness of the sample. The presented values are average of two measurements.

2.9. Water contact angle (CA)

CA of water on pure and coated NFC films were determined using the CAM 200 (KSV Instruments Ltd., Helsinki, Finland) contact angle meter with computer based controlling system and capturing video camera. The static sessile drop method was employed in measurements and CA was determined for at least three spots on each sample. The tests were performed with pure water at room temperature, and droplet volume of 6.7 μl was used. The full Young–Laplace equation was used to determine the contact angle shape of the sessile drop.

2.10. Atomic force microscope imaging (AFM)

AFM imaging in air was used to observe changes in morphology of ultrathin NFC films. The Nanoscope V MultiMode scanning probe microscope (Bruker Corporation, MA, USA) was used in tapping mode. Silicon cantilevers (NSC15/AIBS, MicroMasch, Tallinn, Estonia) with driving frequency around 300–360 kHz were used for imaging. The radius of the tip according to the manufacturer was less than 10 nm. At least three different places on the surface were imaged for each sample. No further processing was applied to images except of flattening.

3. Results and discussion

Up to the present, several methods for the modification of the NFC surface have been described (Dufresne, 2012). In order to

add hydrophobic properties to the naturally hydrophilic fibers, polymerization techniques or esterification reactions were applied. These methods, however, often require the use of organic solvents and hence a tedious solvent exchange from water to the respective organic solvent has to be performed for the NFC. In this paper we describe a method for the modification of NFC using water as a medium and GGM as a carrier of a hydrophobic functionality.

3.1. Synthesis of GGM-block-structured derivatives

Two different kinds of GGM-block-structured derivatives were prepared. The first series of products consists of GGM derivatized with fatty acids. Three fatty acids were used, pelargonic acid (C9), myristic acid (C14), and stearic acid (C18). Before the fatty acids could be used in a reductive amination with GGM, their carboxylic acid group had to be modified and an amino functional group was inserted in a three-step reaction (Dax, Eklund, et al., 2013; Dax, Xu, et al., 2013). The reaction pathway and reaction conditions are schematically shown in Scheme 1 and the detailed reaction parameters can be found in the supporting information. All the intermediate products were characterized with ^{1}H NMR and FTIR. The successful syntheses of the GGM-block structured fatty acid derivatives were proven by ^{1}H and ^{13}C NMR spectra. In Figs. S1 and S2 in the supporting information the disappearance of the reducing end peaks of GGM (at 4.93 and 5.20 ppm) and the simultaneous appearance of the characteristic fatty acid signals can be seen in the ^{1}H NMR spectrum of GGM-*block*-C9 and the dept-135 spectrum of the GGM-*block*-C18.

In order to generate an amphiphilic GGM-block-structured derivative with a longer hydrophobic tail, GGM was converted with a diamino polydimethylsiloxane (NH_2-PDMS-NH_2) with a molar mass of 900 g/mol (Scheme 1). The reaction showed to be challenging because of the solubility differences between GGM and NH_2-PDMS-NH_2 and the need to avoid GGM to precipitate in the solution. A carefully chosen mixture of DMSO and THF in a ratio of 5:2 was successfully used for the reductive amination. It was important to add acid to the NH_2-PDMS-NH_2 solution before the addition to GGM because the basic character of NH_2-PDMS-NH_2 lead to fast and undesired deacetylation of the GGM.

The GGM-*block*-PDMS derivative was analyzed by ^{1}H NMR and the full conversion of the reducing end peak of GGM at 5.20 ppm could be observed (Fig. 1). At the same time the characteristic peaks of the PMDS CH_3 groups in the range from −0.18 to 0.23 ppm emerged. In the final product, two distinguished alkyl chains were present, originating from the NH_2-PDMS-NH_2. To correctly assign the respective signals in the ^{1}H NMR, the CH_2 (H-11) group in the neighborhood of the —NH— was identified to be at 3.12 ppm. This identification was performed by recording a ^{1}H NMR of a GGM-PDMS-GGM derivative in which all the amino groups of NH_2-PDMS-NH_2 reacted and hence only —NH—CH_2— was present, whereas in the GGM-*block*-PDMS derivative there was one —NH—CH_2— and one NH_2—CH_2— group with similar shifts in the ^{1}H spectrum. The CH_2 (H-17) signal next to the unreacted NH_2 was assigned to the peak at 3.01 ppm. By evaluating a 2D COSY spectrum of GGM-*block*-PDMS the Si—CH_2—CH_2—CH_2—NH— (H-12) signal was found to be at 1.77 ppm and the Si—CH_2—CH_2—CH_2—NH_2 (H-16) at 1.71 ppm. The CH_2 groups next to the Si atoms had a similar shift of 0.56 for Si—CH_2—$(CH_2)_2$—NH— (H-13) and 0.55 ppm for Si—CH_2—$(CH_2)_2$—NH_2 (H-15). The acetyl groups (H-7) of GGM could be found at 2.09 ppm. Here it has to be noted that during the chemical modification of GGM, no deacetylation took place.

For all the products, FTIR spectra were recorded and the results for native GGM and GGM-*block*-PDMS are shown in Fig. 3. The spectrum from NH_2-PDMS-NH_2 was recorded as a reference and at 2960 cm^{-1}, the C—H valence vibration signal could be detected (Cai, Neyer, Kuckuk, & Heise, 2010). The C—H bending vibration was

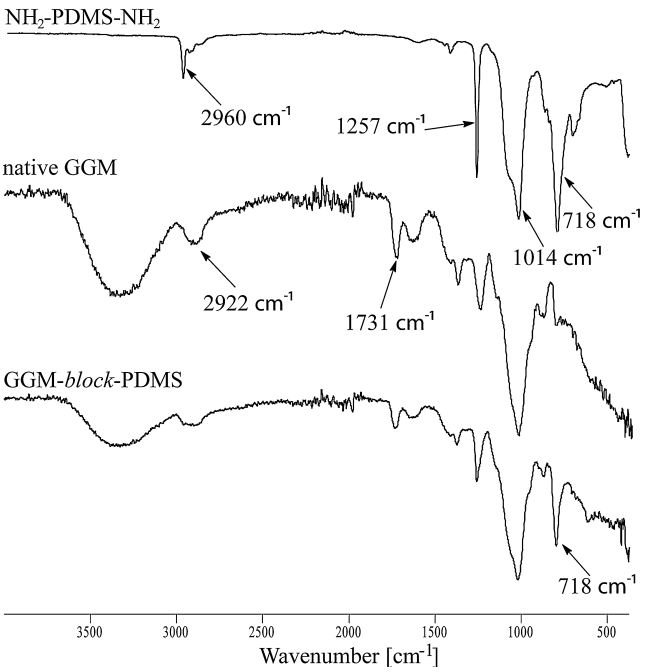

Fig. 3. FTIR spectra of the reagent NH_2-PDMS-NH_2, native GGM and GGM-*block*-PDMS.

assigned to the signal at 1257 cm^{-1} and the Si—O valence vibration was found at 1014 cm^{-1}. Furthermore, the Si—C valence vibration could be separately detected at 718 cm^{-1}. The latter peak is the one that could also be observed in the spectrum of GGM-*block*-PDMS, which tightens the proof of the successful formation of the product. The other signals resulting from the PDMS chain in the GGM derivative could not be separately assigned because they were overlapping with signals originating from the GGM chain. The carbonyl group signal (ν_sC=O) at 1731 cm^{-1} is present in the native GGM spectrum as well as in the GGM-*block*-PDMS arising from the acetyl group.

3.2. Adsorption of GGM and GGM-block-copolymers on NFC

Adsorption of the GGM and its derivatives on ultrathin NFC films was studied in situ with the QCM-D technique in aqueous media. The unmodified GGM and its block-structured derivatives (GGM-*b*-C9, GGM-*b*-C14, GGM-*b*-C18, and GGM-*b*-PDMS) were found to adsorb well on the cellulosic surface. In Fig. 4 the adsorption kinetics are represented as the change in frequency (Δf, 3rd overtone) for NFC coated quartz crystals during adsorption. Larger change in frequency indicates higher adsorbed amount. It can be seen from the adsorption curves that all polymers have rather similar adsorption behavior, with fast and significant adsorption during the first minutes after injection of the solution, followed by subsequent slow saturation of the surface with adsorbate.

After adsorption, the system was rinsed with water to estimate possible detachment of the molecules. In Fig. 4 an increase in frequency after the rinsing could be observed, probably deriving from the removal of only loosely attached molecules from the surface. Nevertheless, the frequency did not increase up to its initial value (0 Hz), meaning that a substantial amount of molecules remained adsorbed to the surface. The estimated sensed mass for each substance after rinsing was calculated using Eq. (1): 2.5 mg/m^2 (unmodified GGM), ~4 mg/m^2 (GGM-*b*-C9, GGM-*b*-C14, and GGM-*b*-C18), and 9.8 mg/m^2 (GGM-*b*-PDMS). Interestingly, the adsorbed mass of each of the fatty acid derivatives; GGM-*b*-C9, GGM-*b*-C14, and GGM-*b*-C18 was practically the same after rinsing, and nearly

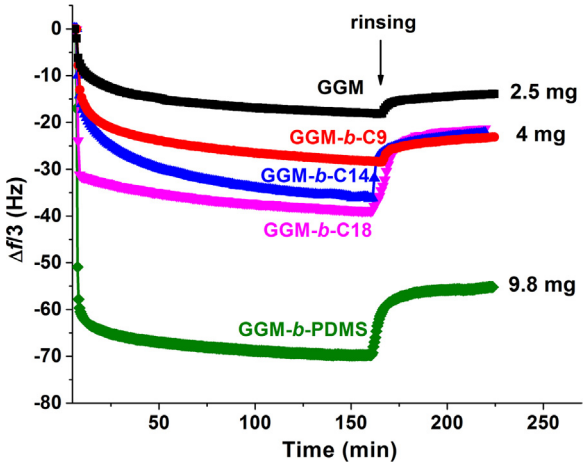

Fig. 4. Change in frequency (Δf_3) with time during adsorption of unmodified GGM, GGM-*b*-C9, GGM-*b*-C14, GGM-*b*-C18, or GGM-*b*-PDMS on NFC substrate from 0.5 g/l aqueous solutions. The polymer was injected at $t = 5$ min. The sensed mass after rinsing, calculated using Eq. (1), is indicated for each sample.

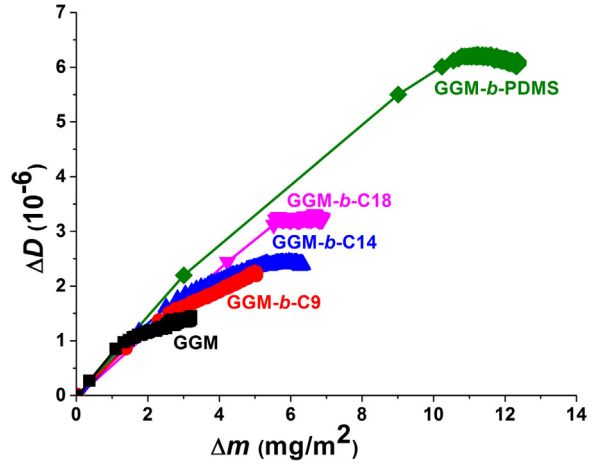

Fig. 5. Change in dissipation (ΔD_3) as a function of adsorbed mass (Δm) during adsorption of unmodified GGM, GGM-*b*-C9, GGM-*b*-C14, GGM-*b*-C18, and GGM-*b*-PDMS on NFC substrate from 0.5 g/l aqueous solutions. Curves excluded rinsing step for clarity purposes and ease in reading the graph. Adsorbed mass was calculated using the Sauerbrey equation (Eq. (1)).

twice as high as the sensed mass of unmodified GGM. However, change in frequency is due to both adsorbed polymer and bound water. GGM, its derivatives, as well as NFC substrate all bind water, therefore the calculated mass reflects not only amount of adsorbed polymer but also associated water. Furthermore, the Sauerbrey equation (Eq. (1)) is not strictly correct for viscoelastic layers with dissipation values higher than 1. Thus the calculated sensed mass should be used for comparison only, not taken as absolute values.

Unmodified GGM adsorbs on NFC due to the natural affinity of hemicelluloses toward cellulose (Eronen et al., 2011). This inherent affinity is likely to play a role also in case of the studied GGM derivatives, due to the preserved structure of the GGM backbone. Although hydrogen bonding usually is not the driving force for adsorption in water, it does play a role during adsorption of polysaccharides on cellulose, as recently shown by Kargl et al. (2012). Due to their similar structure, GGM can come in close contact with the cellulose and multiple hydrogen bonds are formed. Moreover, it must be remembered that not only the interaction between solute and surface play a role during adsorption, but also the interaction between solvent and solute. Thus the hydrophobicity of the fatty acid and PDMS blocks also promotes adsorption, this effect being stronger the higher the molar mass of the hydrophobic block. Moreover, if the amount of adsorbed molecules would be the same, higher molar mass would give higher sensed mass. It can be seen from Fig. 4 that the magnitude of the initial adsorption of block-copolymers increases with an increase in chain length of the hydrophobic part (chain length of the fatty acids C9, C14, and C18 respectively). The solubility and adsorption of the GGM-*b*-PDMS derivative might also be affected by the presence of amine group in its structure. But since there is only one group in a big molecule, we consider its influence to be rather insignificant.

The synthesized block-co-polymers are amphiphilic and thus able to form micelles in solution. Corresponding CMC values were determined for each polymer and are presented in Table 1.

For all QCM-D experiments, the concentration of the solution was 0.5 g/l, which is below the CMC values for the amphiphilic polymers used in this study, therefore GGM derivatives in solution were not present in the form of micelles. To understand adsorption mechanisms of GGM and derivatives on the NFC surface the energy dissipation as a function of adsorbed mass was plotted in Fig. 5.

In Fig. 5, linear increase in mass and dissipation corresponds to the first few minutes of the adsorption process (further referred to as first or initial step). We propose that during this time the GGM derivatives adsorbed due to affinity between NFC and the hemicellulosic part of the adsorbed molecules. In this way a swollen viscoelastic monolayer of GGM derivatives was formed on top of the NFC film. Further small but continuous mass uptake can be observed and as an explanation we suggest the formation of a bilayer structure due to the aggregation of hydrophobic blocks (further referred as second step). The structure of the GGM derivatives and the proposed mechanism of the bilayer formation are presented in Fig. 6.

Depending on the adsorbed molecule, certain differences were found in the viscoelastic properties of the formed films. GGM formed a rather strongly bound layer in flat conformation on the NFC surface. After the initial adsorption step, adsorption of the GGM continued slowly. However, adsorption became reversible after a certain amount of GGM was adsorbed, when molecules no longer could bind strongly to the surface. Therefore some material was removed during rinsing. We speculate that in contrast to pure GGM, the GGM derivatives, with their amphiphilic nature, form a bilayer structure, resulting in a more swollen and dissipative layer. Interestingly, the dissipation values did not increase with increase in mass during the second step of the adsorption process for GGM-*b*-C14 and GGM-*b*-C18 (plateau in the $\Delta D/\Delta m$ curve). This indicates that the bilayer became more rigid. The NFC film contained a substantial amount of bound water and also GGM and its derivatives are assumed to bind water due to their hydrophilicity. However, the coupled water is likely to be removed from the cellulosic network during the bilayer formation on the NFC surface. As for GGM-*b*-PDMS, the dissipation value is reaching a peak and decreasing slowly hereafter. Possible reasons for this phenomenon are changes in conformation of the polymers during the second step of the adsorption, mainly densification of the

Table 1
CMC values of synthesizes block-copolymers.

	CMC (g/l)
GGM-*b*-C9	2.44
GGM-*b*-C14	1.82
GGM-*b*-C18	0.88
GGM-*b*-PDMS	2.78

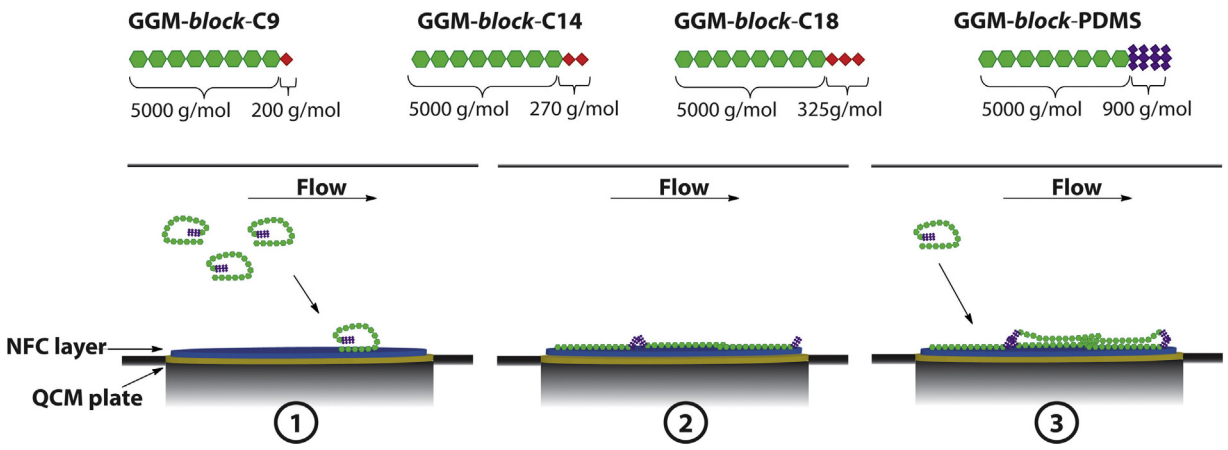

Fig. 6. Molar mass and schematic structure of amphiphilic block-copolymers (GGM-*b*-C9, GGM-*b*-C14, GGM-*b*-C18, and GGM-*b*-PDMS). Schematic illustration of the possible change in conformation and build-up of a bilayer during adsorption of amphiphilic block-copolymers on NFC illustrated with GGM-*b*-PDMS on NFC surface. (1) Adsorption of the entangled GGM-*b*-PDMS on NFC; (2) formation of a viscoelastic layer; and (3) build-up of bilayer.

adsorbed layer and displacement of water from the network. Such reorganization would result in a less swollen and more densely packed block-copolymer layer on top of the NFC film.

As was mentioned before, the adsorbed mass of the GGM-*b*-fatty acid derivatives is about twice as high as the adsorbed mass of pure GGM. This observation correlates well with our hypothesis about bilayer formation when amphiphilic derivatives are adsorbed. Whereas the large adsorbed mass of GGM-*b*-PDMS can be attributed to the high molar mass of the copolymer, as was mentioned earlier.

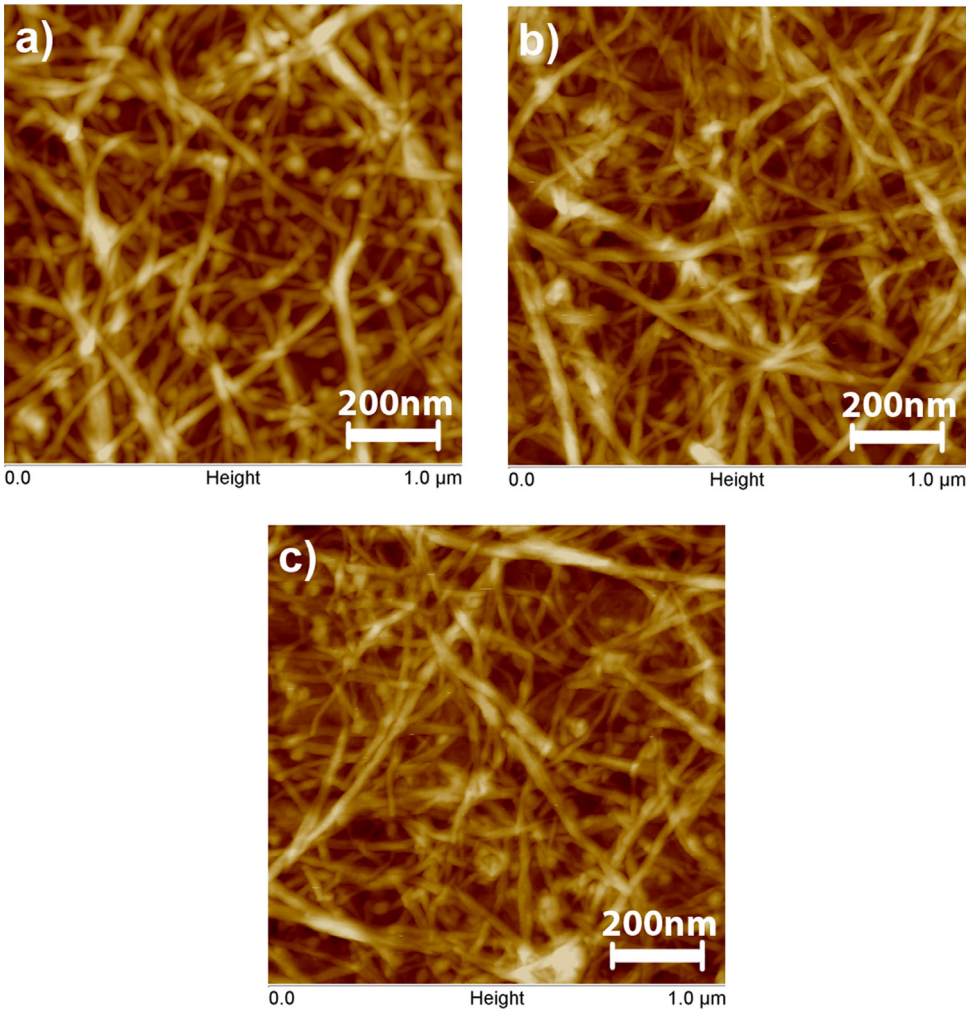

Fig. 7. AFM height images of pure NFC thin film on QCM-D crystal (a) and GGM-*b*-PDMS adsorbed on NFC film below (b) and above (c) the CMC. The images were scanned in air.

Table 2
Oxygen permeability and water contact angle of pure and coated NFC films.

		OP 0% RH (cc μm/m^2 day kPa)	OP 80% RH (cc μm/m^2 day kPa)	CA(°) after 0.2 s
NFC		0.4	11.7	30
NFC+	GGM	0.4	9.0	13
	GGM-*b*-C9	0.5	17.4	40
	GGM-*b*-C14	0.1	9.4	25
	GGM-*b*-C18	0.3	6.2	33
	GGM-*b*-PDMS	0.1	8.9	60

3.3. Morphology of NFC thin films

In Fig. 7, AFM height images of ultrathin NFC films before and after adsorption of (GGM-*b*-PDMS) are shown. The amphiphilic polymer was adsorbed at concentrations below and above CMC, but no micelles were visible on the NFC surface even after adsorption above CMC. This is probably due to break down of the micelles during adsorption process or during the drying of the sample prior to imaging.

3.4. Oxygen barrier properties and hydrophobicity of coated NFC films

Pure NFC films have shown excellent oxygen barriers properties, especially at low relative humidity values (Lee et al., 2012; Liu, Walther, Ikkala, Belova, & Berglund, 2011; Österberg et al., 2013). Furthermore, hydrophobic modification of the fibrils prior to film formation often lead to poor barrier properties due to poor bonding between the fibrils. Thus, surface modification of NFC films has been suggested as an efficient route to enhance barrier properties at elevated humidity (Hirvikorpi, Vähä-Nissi, Nikkola, Harlin, & Karppinen, 2011; Österberg et al., 2013). In this work the possibility to further improve barrier properties of the NFC film with polysaccharides derivatives was explored. Oxygen permeability of pure self-standing NFC film and NFC films coated with GGM and amphiphilic GGM derivatives are presented in Table 2. At dry conditions there was no significant difference between the samples and all films had very low OP, as expected for NFC films. Amphiphilic GGM derivatives were expected to decrease the OP at high relative humidity and increase hydrophobicity of the NFC film, due to the presence of hydrophobic groups in synthesized block-copolymer. However, although a clear trend as a function of chain length is noted for the fatty acid derivatives, the change compared to pure NFC is not significant. The water contact angle results further support this finding. Only the GGM-*b*-PDMS was able to significantly increase the contact angle and for most of the GGM samples the hydrophilicity actually increased by addition of GGM.

It should be noted, that CA values were found to vary ±10° for duplicate samples during measurements, this can be referred to the varied reactivity of the NFC film after drying (Johansson et al., 2011). It is important to mention that the water droplet penetrated samples coated with GGM, GGM-*b*-C9; GGM-*b*-C14, or GGM-*b*-C18 within 2–5 s. Therefore, we can conclude that the short fatty acid chain, compared to the hydrophilic GGM part is not enough to introduce significant hydrophobicity to the NFC surface, and moreover, the use of mentioned copolymers facilitates water uptake due to the hydrophilic nature of GGM. In contrast, the drop stays on the surface and penetrates rather slowly into the film on pure NFC and NFC-*b*-PDMS coated samples. Hence, in the case when the GGM-*b*-PDMS copolymer is applied as a surfactant, the PDMS appears to be large enough to increase the hydrophobicity of the sample.

It was speculated that the amphiphilic GGM derivatives formed bilayers on the NFC ultrathin films and consequently bilayers could form on self-standing NFC film during spin-coating. Bilayer formation is well known to decrease the water contact angle since the hydrophilic part of the polymer is exposed (Wang, Gu, Liang, & Hamilton, 2004). But this structure even if formed, is likely to change during hot pressing of the film after spin-coating. Results of this study show, that hydrophobicity can be introduced to cellulosic surface if the modification is done in the right way. Thus, large enough hydrophobic segments should be introduced to the GGM molecule, while the solubility of the GGM derivatives in water is still preserved.

4. Conclusion

In this work, a method to modify NFC surfaces in aqueous media using amphiphilic GGM derivatives is proposed. The modified GGM is still water-soluble and adsorbs irreversibly onto NFC and the adsorption and layer properties can be monitored by QCM-D. The block-structure of the derivatives gives the derivatives unique properties. They behave as surfactants in solution and can form bilayer structures when adsorbed on cellulose. The different GGM derivatives can be used to modify the surface of NFC films but it is challenging to enhance hydrophobicity using modified hydrophilic polysaccharides as long as the hydrophilic GGM part of the molecule dominates the properties. However, using GGM-*b*-PDMS, the presence of the highly hydrophobic tail with higher molecular molar mass improves the hydrophobicity of the cellulosic surface modified with the derivative. Overall, the results of the experiments lead to the conclusion that GGM is a suitable carrier of functional molecules and can be applied to introduce different functionalities to NFC. The gained knowledge can be exploited in further experiments, so for example GGM's with different molar masses could be used as starting materials. Synthesized copolymers with fatty acids can have a positive effect on the compatibility of NFC in novel biocomposites. Furthermore, GGM-*b*-PDMS might reduce aggregation of NFC and contribute to better distribution in non-polar solvents.

Acknowledgements

Ms. Ritva Kivelä and Mr. Xi Chen are acknowledged for NFC films preparation. Daniel Dax thanks the National Research Fund of Luxembourg (AFR) for granting him a scholarship. The Graduate School of Biomass Refining (BIOREGS) is thanked for financial support. Chunlin Xu thanks the funding from Knut and Alice Wallenberg Foundation via Wallenberg Wood Science Center, Sweden. This work was also part of the activities at the Åbo Akademi Process Chemistry Centre. Alina Lozhechnikova acknowledges Aalto University for funding through the WoodLife project.

Appendix A. Supplementary data

Supplementary data associated with this article can be found, in the online version, at http://dx.doi.org/10.1016/j.carbpol.2014.03.087.

References

Ahola, S., Salmi, J., Johansson, L.-S., Laine, J., & Österberg, M. (2008). Model films from native cellulose nanofibrils. Preparation swelling, and surface interactions. *Biomacromolecules*, *9*, 1273–1282.

Al Manasrah, M., Kallioinen, M., Ilvesniemi, H., & Mänttäri, M. (2012). Recovery of galactoglucomannan from wood hydrolysate using regenerated cellulose ultrafiltration membranes. *Bioresource Technology*, *114*, 375–381.

Albertsson, A.-C., Voepel, J., Edlund, U., Dahlman, O., & Söderqvist-Lindblad, M. (2010). Design of renewable hydrogel release systems from fiberboard mill wastewater. *Biomacromolecules*, *11*(1406–1411), 1406.

Andresen, M., & Stenius, P. (2007). Water-in-oil emulsions stabilized by hydrophobized microfibrillated cellulose. *Journal of Dispersion Science and Technology*, *28*(6), 837–844.

Andresen, M., Stenstad, P., Moretro, T., Langsrud, S., Syverud, K., Johansson, L.-S., et al. (2007). Nonleaching antimicrobial films prepared from surface-modified microfibrillated cellulose. *Biomacromolecules*, *8*(2149–2155), 2149.

Cai, D., Neyer, A., Kuckuk, R., & Heise, H. M. (2010). Raman, mid-infrared, near-infrared and ultraviolet–visible spectroscopy of PDMS silicone rubber for characterization of polymer optical waveguide materials. *Journal of Molecular Structure*, *976*, 274–281.

Dax, D., Eklund, P., Hemming, J., Sarfraz, J., Backman, P., Xu, C., et al. (2013). Amphiphilic spruce galactoglucomannan derivatives based on naturally-occurring fatty acids. *BioResources*, *8*(3), 3771–3790.

Dax, D., Xu, C., Långvik, O., Hemming, J., Backman, P., & Willför, S. (2013). Synthesis of SET-LRP-induced galactoglucomannan-diblock copolymers. *Journal of Polymer Science Part A: Polymer Chemistry*, *51*(23), 5100–5110.

Dufresne, A. (2012). *Chemical modification of nanocellulose. Nanocellulose: From nature to high performance tailored materials*. Berlin, Boston, MA: De Gruyter.

Eronen, P., Österberg, M., Heikkinen, S., Tenkanen, M., & Laine, J. (2011). Interactions of structurally different hemicelluloses with nanofibrillar cellulose. *Carbohydrate Polymers*, *86*(3), 1281–1290.

Filpponen, I., Kontturi, E., Nummelin, S., Rosilo, H., Kolehmainen, E., Ikkala, O., et al. (2012). Generic method for modular surface modification of cellulosic materials in aqueous medium by sequential "click" reaction and adsorption. *Biomacromolecules*, *13*(3), 736–742.

Hannuksela, T., & Hervé du Penhoat, C. (2004). NMR structural determination of dissolved O-acetylated galactoglucomannan isolated from spruce thermomechanical pulp. *Carbohydrate Research*, *339*(2), 301–312.

Hirvikorpi, T., Vähä-Nissi, M., Nikkola, J., Harlin, A., & Karppinen, M. (2011). Thin Al_2O_3 barrier coatings onto temperature-sensitive packaging materials by atomic layer deposition. *Surface and Coatings Technology*, *205*(21–22), 5088–5092.

Höök, F., Kasemo, B., Nylander, T., Fant, C., Sott, K., & Elwing, H. (2001). Variations in coupled water, viscoelastic properties, and film thickness of a Mefp-1 protein film during adsorption and cross-linking: A quartz crystal microbalance with dissipation monitoring, ellipsometry, and surface plasmon resonance study. *Analytical Chemistry*, *73*(24), 5796–5804.

Hubbe, M. A., Rojas, O. J., Lucia, L. A., & Sain, M. (2008). Cellulosic nanocomposites: A review. *BioResources*, *3*(3), 929–980.

Johansson, L.-S., Tammelin, T., Campbell, J. M., Setälä, H., & Österberg, M. (2011). Experimental evidence on medium driven cellulose surface adaptation demonstrated using nanofibrillated cellulose. *Soft Matter*, *7*(22), 10917–10924.

Kargl, R., Mohan, T., Bracic, M., Kulterer, M., Doliska, A., Stana-Kleinschek, K., et al. (2012). Adsorption of carboxymethyl cellulose on polymer surfaces: Evidence of a specific interaction with cellulose. *Langmuir*, *28*(31), 11440–11447.

Kisonen, V., Eklund, P., Auer, M., Sjöholm, R., Pranovich, A., Hemming, J., et al. (2012). Hydrophobication and characterisation of O-acetyl-galactoglucomannan for papermaking and barrier applications. *Carbohydrate Research*, *352*, 151–158.

Klemm, D., Heublein, B., Fink, H. P., & Bohn, A. (2005). Cellulose: Fascinating biopolymer and sustainable raw material. *Angewandte Chemie International Edition (English)*, *44*(22), 3358–3393.

Lacerda, P. S., Barros-Timmons, A. M., Freire, C. S., Silvestre, A. J., & Neto, C. P. (2013). Nanostructured composites obtained by ATRP sleeving of bacterial cellulose nanofibers with acrylate polymers. *Biomacromolecules*, *14*(6), 2063–2073.

Lee, K.-Y., Tammelin, T., Schulfter, K., Kiiskinen, H., Samela, J., & Bismarck, A. (2012). High performance cellulose nanocomposites: Comparing the reinforcing ability of bacterial cellulose and nanofibrillated cellulose. *ACS Applied Materials & Interfaces*, *4*(8), 4078–4086.

Littunen, K., Hippi, U., Johansson, L.-S., Österberg, M., Tammelin, T., Laine, J., et al. (2011). Free radical graft copolymerization of nanofibrillated cellulose with acrylic monomers. *Carbohydrate Polymers*, *84*(3), 1039–1047.

Liu, A., Walther, A., Ikkala, O., Belova, L., & Berglund, L. A. (2011). Clay nanopaper with tough cellulose nanofiber matrix for fire retardancy and gas barrier functions. *Biomacromolecules*, *12*(3), 633–641.

Lundqvist, J., Jacobs, A., Palm, M., Zacchi, G., Dahlman, O., & Stålbrand, H. (2003). Characterization of galactoglucomannan extracted from spruce (*Picea abies*) by heat-fractionation at different conditions. *Carbohydrate Polymers*, *51*, 203–211.

Moon, R. J., Martini, A., Nairn, J., Simonsen, J., & Youngblood, J. (2011). Cellulose nanomaterials review: Structure, properties and nanocomposites. *Chemical Society Reviews*, *40*(7), 3941–3994.

Olszewska, A., Junka, K., Nordgren, N., Laine, J., Rutland, M. W., & Österberg, M. (2013). Non-ionic assembly of nanofibrillated cellulose and polyethylene glycol grafted carboxymethyl cellulose and the effect of aqueous lubrication in nanocomposite formation. *Soft Matter*, *9*(31), 7448–7457.

Österberg, M., Vartiainen, J., Lucenius, J., Hippi, U., Seppälä, J., Serimaa, R., et al. (2013). A fast method to produce strong NFC films as a platform for barrier and functional materials. *ACS Applied Materials & Interfaces*, *5*(11), 4640–4647.

Parikka, K., Leppänen, A. S., Xu, C., Pitkänen, L., Eronen, P., Österberg, M., et al. (2012). Functional and anionic cellulose-interacting polymers by selective chemo-enzymatic carboxylation of galactose-containing polysaccharides. *Biomacromolecules*, *13*(8), 2418–2428.

Pääkkö, M., Ankerfors, M., Kosonen, H., Nykänen, A., Ahola, S., Österberg, M., et al. (2007). Enzymatic hydrolysis combined with mechanical shearing and high-pressure homogenization for nanoscale cellulose fibrils and strong gels. *Biomacromolecules*, *8*, 1934–1941.

Sauerbrey, G. (1959). Verwendung von Schwingquarzen zur Wägung dünner Schichten und zur Mikrowägung. *Zeitschrift für Physik*, *155*(2), 206–222.

Schatz, C., & Lecommandoux, S. (2010). Polysaccharide-containing block copolymers: Synthesis, properties and applications of an emerging family of glycoconjugates. *Macromolecular Rapid Communications*, *31*(19), 1664–1684.

Stenstad, P., Andresen, M., Tanem, B., & Stenius, P. (2008). Chemical surface modifications of microfibrillated cellulose. *Cellulose*, *15*(1), 35–45.

Svagan, A. J., Azizi Samir, M. A. S., & Berglund, L. A. (2007). Biomimetic polysaccharide nanocomposites of high cellulose content and high toughness. *Biomacromolecules*, *8*, 2556–2563.

Swerin, A., Ödberg, L., & Lindström, T. (1990). Deswelling of hardwood kraft pulp fibers by cationic polymers: The effect on wet pressing and sheet properties. *Nordic Pulp and Paper Research Journal*, *5*(4), 188–196.

Taipale, T., Österberg, M., Nykänen, A., Ruokolainen, J., & Laine, J. (2010). Effect of microfibrillated cellulose and fines on the drainage of kraft pulp suspension and paper strength. *Cellulose*, *17*(5), 1005–1020.

Voepel, J., Edlund, U., Albertsson, A.-C., & Percec, V. (2011). Hemicellulose-based multifunctional macroinitiator for single-electron-transfer mediated living radical polymerization. *Biomacromolecules*, *12*, 253–259.

Wågberg, L., Decher, G., Norgren, M., Lindström, T., Ankerfors, M., & Axnäs, K. (2008). The build-up of polyelectrolyte multilayers of microfibrillated cellulose and cationic polyelectrolytes. *Langmuir*, *24*, 784–795.

Wågberg, L., Enarsson, L.-E., & Österberg, M. (2010). *Interactions at cellulose model surfaces. Encyclopedia of surface and colloid science* (2nd ed., pp. 1–19). London, UK: Taylor & Francis.

Wang, M., Olszewska, A., Walther, A., Malho, J. M., Schacher, F. H., Ruokolainen, J., et al. (2011). Colloidal ionic assembly between anionic native cellulose nanofibrils and cationic block copolymer micelles into biomimetic nanocomposites. *Biomacromolecules*, *12*(6), 2074–2081.

Wang, W., Gu, B., Liang, L., & Hamilton, W. A. (2004). Adsorption and structural arrangement of cetyltrimethylammonium cations at the silica nanoparticle–water interface. *The Journal of Physical Chemistry B*, *108*(45), 17477–17483.

Willför, S., Sjöholm, R., Laine, C., Roslund, M., Hemming, J., & Holmbom, B. (2003). Characterisation of water-soluble galactoglucomannans from Norway spruce wood and thermomechanical pulp. *Carbohydrate Polymers*, *52*, 175–187.

Yamanaka, S., Watanabe, K., & Kitamura, N. (1989). The structure and mechanical properties of sheets prepared from bacterial cellulose. *Journal of Materials Science*, *24*, 3141–3145.